Biochimica et Biophysica Acta 1807 (2011) 1056–1063

Contents lists available at ScienceDirect

Biochimica et Biophysica Acta

journal homepage: www.elsevier.com/locate/bbabio

Carotenoids are essential for normal levels of dimerisation of the RC–LH1–PufX core complex of *Rhodobacter sphaeroides*: Characterisation of R-26 as a *crtB* (phytoene synthase) mutant

Irene W. Ng, Peter G. Adams, David J. Mothersole, Cvetelin Vasilev, Elizabeth C. Martin, Helen P. Lang, Jaimey D. Tucker, C. Neil Hunter *

Department of Molecular Biology and Biotechnology, University of Sheffield, Sheffield S10 2TN, UK

ARTICLE INFO

Article history:
Received 11 March 2011
Received in revised form 18 May 2011
Accepted 23 May 2011
Available online 30 May 2011

Keywords:
Bacterial photosynthesis
Light-harvesting
Membrane protein
Photosynthetic membrane
Carotenoid
Atomic force microscopy

ABSTRACT

Carotenoids play important roles in photosynthesis where they are involved in light-harvesting, in photo-protection and in the assembly and structural stability of light-harvesting and reaction centre complexes. In order to examine the effects of carotenoids on the oligomeric state of the reaction centre–light-harvesting 1 -PufX (RC–LH1–PufX) core complex of *Rhodobacter sphaeroides* two carotenoid-less mutants, TC70 and R-26, were studied. Detergent fractionation showed that in the absence of carotenoids LH2 complexes do not assemble, as expected, but also that core complexes are predominantly found as monomers, although levels of the PufX polypeptide appeared to be unaffected. Analysis of R-26 membranes by electron microscopy and atomic force microscopy reveals arrays of hexagonally packed monomeric RC–LH1–PufX complexes. Transfer of the *crtB* gene encoding phytoene synthase to TC70 and R-26 restores the normal synthesis of carotenoids demonstrating that the R-26 mutant of *Rba. sphaeroides* harbours a mutation in *crtB*, among its other defects. The transconjugant TC70 and R-26 strains containing *crtB* had regained their ability to assemble wild-type levels of dimeric RC–LH1–PufX core complexes and normal energy transfer pathways were restored, demonstrating that carotenoids are essential for the normal assembly and function of both the LH2 and RC–LH1–PufX complexes in this bacterial photosystem.

1. Introduction

Carotenoids serve three functions in photosynthetic organisms: they act as accessory light-harvesting pigments, they protect the bacterial cell from the damaging effects of reactive oxygen species (ROS) generated during cell metabolism, and finally they play a role in the assembly and structural stability of photosynthetic complexes. The work of Thomas [1] was possibly the first to demonstrate the role of carotenoids in bacterial photosynthesis, by measuring maxima at 460, 490 and 525 nm for the action spectrum of photosynthesis in whole cells of *Rhodospirillum* (*Rsp.*) *rubrum*. The isolation and extensive analysis of a pale blue *carotenoid-less* mutant, UV-33, of *Rhodobacter* (*Rba.*) *sphaeroides* (then *Rhodopseudomonas spheroides*) definitively established that carotenoids play an essential role in preventing photo-oxidative damage, as well as in establishing the normal characteristics of *in vivo* bacteriochlorophyll (BChl) absorption [2]. Subsequently, Clayton and Smith isolated a carotenoid-less mutant, R-26 (originally CC1 R26), following exposure of a high catalase mutant, isolated from continuous cultures grown in the presence of 0.1 M H_2O_2, to ultraviolet light [3]. The aim of their study was to determine whether the loss of carotenoids, and therefore photo-protection, could be compensated by increasing the catalase content, although their results showed that the high catalase content provided no protection against the photo-oxidative killing.

Following the earlier work of Duysens, who had demonstrated reversible light-dependent changes in the BChl absorption spectrum in whole cells of *Rsp. rubrum* [4], studies on *carotenoid-less* mutants played a central role in the history of photosynthesis research. Clayton studied reversible light-induced changes in absorption in mutants R-26 and UV-33 and proposed that the photochemical reactions of photosynthesis arise from the reversible *photo-oxidation* of a small subset of pigments, designated $BChl_2$ [5]. R-26 was used for investigations into the nature of this reversible component, P870 [6], and then for the first isolation of reaction centres (RCs) [7,8]. Subsequently R-26 RCs were crystallised [9–11] providing some of the first insights into the structure of RC complexes, following the structural work on the RC from *Rhodopseudomonas viridis* [12]. The simplified light-harvesting system of R-26, which lacked LH2, was

Abbreviations: AFM, atomic force microscopy; BChl(s), bacteriochlorophyll(s); EDTA, ethylenediamine tetraacetic acid; HEPES, N-2-hydroxyethylpiperazine-N′-2-ethanesulfonic acid; ICM, intracytoplasmic membrane; LH1, light-harvesting 1 complex; LH2, light-harvesting 2 complex; NIR, near-infrared; *Rba.*, *Rhodobacter*; RC, reaction centre; RC–LH1, reaction centre–light-harvesting 1; *Rsp.*, *Rhodospirillum*; SDS-PAGE, sodium dodecyl sulphate polyacrylamide gel electrophoresis; Tris, Tris (hydroxymethyl)aminomethane; β-DDM, β-dodecylmaltoglucoside

* Corresponding author. Tel.: +44 114 222 4191; fax: +44 114 222 2711.
E-mail address: c.n.hunter@sheffield.ac.uk (C. Neil Hunter).

0005-2728/$ – see front matter © 2011 Elsevier B.V. All rights reserved.
doi:10.1016/j.bbabio.2011.05.020

also an attractive experimental system for analysis of antenna complexes (for example, Ref. [13]).

The loss of coloured carotenoids not only has implications for the cell in terms of light-harvesting and photo-protection, but the mutation also provokes structural effects resulting in the absence of LH2 from the intracytoplasmic membrane (ICM) [2,5,14–17]. It was shown that LH2 polypeptides are synthesised but not incorporated into the membrane when either the *crtB* or *crtI* gene, encoding phytoene synthase or phytoene desaturase, respectively (Fig. 1), is interrupted; complementation of this mutant with a plasmid containing a functional copy of this gene resulted in restoration of assembly of the LH2 complex [18]. Given the importance of carotenoids for biosynthesis of the LH2 complex, we looked for a role for carotenoids in the assembly of the other major component of the photosynthetic apparatus in *Rba. sphaeroides*, the RC–LH1–PufX complex. This dimeric structure [19–21] is composed of 28 LH1 αβ polypeptide pairs that snake round two RCs, and which coordinate 56 BChl molecules [22]. The first isolation and analysis of the LH1 complex from *Rba. sphaeroides* had demonstrated a carotenoid:BChl molar ratio of ~1 [23], implying that there could be as many as 56 LH1 carotenoid molecules in the RC–LH1–PufX dimer. Thus, it might be expected that the loss of carotenoids would indeed provoke some rearrangement of the complex, even though it retains its ability to function.

Restoration of normal carotenoid biosynthesis to mutant R-26 was the original motivation for the present work. The carotenoid biosynthesis gene cluster of *Rba. sphaeroides* has been mapped using transposon Tn*5* mutagenesis [17,24,25], then sequenced [17,26], providing defined carotenoid biosynthesis mutants as well as the means to complement the various insertional *crt* mutants. The pale blue phenotype of UV-33, for example Ref. [2], as well as the synthesis of phytoene, can be explained by a mutation in phytoene desaturase, encoded by the *crtI* gene. A lesion in *crtI* is also likely to be the origin of the phytoene-producing phenotype of the CC1 R22 mutant reported by Clayton and Smith [3]. In the same work it was reported that phytoene was absent from the R-26 mutant, so it was likely at the outset that R-26 harbours a mutation in *crtB,* encoding phytoene synthase [16–18,27].

In the work presented herein carotenoid biosynthesis was restored to R-26, showing that it is indeed a *crtB* mutant. The spectroscopic properties of R-26 and the complemented R-26 strain show that the carotenoids are in a functional state, and that energy transfer to BChls is restored, along with LH2 assembly. The oligomeric state of detergent treated carotenoid-less core complexes was analysed by fractionation on sucrose gradients, showing greatly impaired dimer formation in the absence of carotenoids. Membranes from R-26 were analysed by transmission electron microscopy (TEM) and atomic force microscopy (AFM) showing that the loss of carotenoids, as well as abolishing the assembly of LH2, also produces a photosynthetic apparatus largely composed of hexagonally packed, monomeric core complexes. Thus, carotenoids are essential for the normal assembly of both types of photosynthetic complex, LH2 and the RC–LH1–PufX dimer, in *Rba. sphaeroides*.

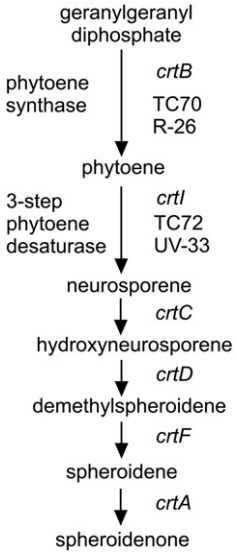

Fig. 1. The carotenoid biosynthetic pathway in *Rba. sphaeroides*. This is a simplified pathway adapted from Ref. [49] and Ref. [50], showing the genes encoding the various steps in the pathway, and the steps that are affected by the TC70, TC72, R-26 and UV-33 mutations.

2. Materials and methods

2.1. Construction of strains

The *crtB* gene was amplified by PCR and cloned into the non-integrative, self-replicating plasmid pRKSK1 [28] to give plasmid pHLKPS1, which was introduced into R-26 and the *crtB* transposon Tn*5* mutant TC70 by conjugative transfer, essentially as described previously [29].

2.2. Growth of cells

The carotenoid-less mutants R-26 and TC70 were grown photosynthetically by inoculating 30 mL screw-topped bottles with colonies picked from plates incubated anaerobically in the light, then subculturing into 1 L bottles immersed in a temperature controlled water bath. Newly inoculated bottles were incubated for a few hours at 30 °C in the dark to remove any residual oxygen, prior to irradiation for photosynthetic growth at 100 μmol m^{-2}. The respective complemented strains R-26[pHLKPS1] and TC70[pHLKPS1], as well as the wild-type (WT), were grown photosynthetically as above but with no preincubation in the dark.

2.3. Sequencing of the crtB gene from R-26

CrtB was sequenced as depicted in Supplementary Fig. S1, which shows the primers used, their positions in relation to *crtB* and the mutation identified in the CrtB primary sequence.

2.4. Preparation of intracytoplasmic membranes

ICMs were prepared as described in Ref. [30], from cells disrupted in a French pressure cell at 18,000 p.s.i. and the cell-free extract layered onto a discontinuous (20/40% w/w) sucrose gradient, which was centrifuged in a Beckman SW32 rotor at 89,500*g* for 10 h. The ICM fraction formed a band above the 20/40% interface, and was collected using a peristaltic pump and stored at −20 °C until required. For AFM and TEM measurements of R-26 membranes, ICMs were further fractionated on a continuous (10–40% w/w) sucrose gradient containing 20 mM HEPES (pH 7.5), 10 mM EDTA by centrifugation at 200,000*g* for 8 h in a Beckman SW41 rotor. The pigmented fraction at 25–30% sucrose was harvested and stored at −20 °C until required. For AFM of wild-type membranes, ICMs were instead fractionated on a continuous (10–40% w/w) sucrose gradient containing 20 mM HEPES (pH 7.5), 5 mM EDTA and 0.02% β-dodecylmaltoglucoside (β-DDM) (Glycon Biochemistry, GmbH Biotechnology, Germany).

2.5. Atomic force microscopy

Atomic force microscopy (AFM) was carried out as previously described in Ref. [30]. Briefly, fractionated ICM was adsorbed onto

freshly cleaved mica in an adsorption buffer of 10 mM HEPES (pH 7.5), 150 mM KCl, 25 mM $MgCl_2$ for 1.5 h, then exchanged into imaging buffer (10 mM HEPES pH 7.5, 100 mM KCl). All imaging was performed using a commercial Nanoscope IV AFM (Bruker, formerly Veeco) in Tapping Mode under imaging buffer, using sharpened silicon nitride cantilevers (Olympus). Imaging parameters were optimised whilst scanning and topographs were recorded at 512×512 pixels and processed using the Nanoscope software (Bruker).

2.6. Transmission electron microscopy of membranes

Fractionated ICMs were applied to glow-discharged carbon-coated copper grids (400 mesh, Agar Scientific), negatively stained with 0.75% (w/v) uranyl formate and examined with a Phillips CM100 electron microscope. Images were recorded using an in-line 1K Gatan Multiscan 794 CCD camera.

2.7. Analysis of monomer/dimer content of membranes using sucrose gradients

ICMs at an absorbance of 15 at 875 nm (1 cm pathlength) were solubilised in a final volume of 250 μL using 3% w/v β-DDM. Following solubilisation each ICM sample was loaded onto a discontinuous sucrose gradient composed of steps of 20%, 21.25%, 22.5%, 23.75% and 25% w/w sucrose (made with 20 mM HEPES, 0.03% β-DDM, pH 7.5), each at a volume of 2 mL. The gradients were centrifuged at 100,000g for 40 h using a Beckman SW41 rotor. The dimer and monomer content of the WT and TC70 was quantified by measuring the absorbance spectra of fractions recovered from gradients and estimating the absorbance values at 870 nm arising from the LH1 complex within the monomer and dimer fractions. The dimer:monomer ratio was estimated separately using densitometry of photographs of the gradients. The original image, containing the two gradients photographed together, was converted to 16-bit greyscale type by using ImageJ software (NIH, Bethesda, USA) and a cross-section profile along the centre-line of the gradient was taken for each sample. The profiles were then exported as ASCII files into Origin software (OriginLab Corp., Northampton, USA) for further analysis. A non-smoothing base line was subtracted from each dataset in order to normalise all the profiles. Then, the peaks corresponding to the pigmented bands of each sample were automatically detected by the software and integrated in order to calculate the area under each peak, providing a measure of the amounts of monomer and dimer complexes in the gradient.

2.8. Spectroscopy

Samples were cooled to 77 K in an Optistat DN-V optical cryostat manufactured by Oxford Instruments. Samples were suspended in a cryo-stable buffer comprising of 50 mM Tris–HCl, 55% glycerol (v/v) 25% sucrose (w/v). Absorbance spectra were recorded on a Cary 50 UV-Vis spectrophotometer between 260 and 950 nm. Baselines were corrected and spectra were processed with Datamax/Grams 32 software as required (Jobin Yvon Ltd., U.S.A.). All emission and excitation fluorescence spectra were recorded on a SPEX FluoroLog spectrofluorimeter (SPEX Industries Inc.). For fluorescence emission measurements excitation slit widths of 5 mm (18 nm) and emission slit widths of 2.5 mm (9 nm) were used. Excitation was provided from a tungsten light source in the visible and near-infrared (NIR) regions of the spectrum. Excitation spectra in the visible and NIR regions were recorded separately since emission was monitored at 910 and 950 nm, respectively. Excitation slit widths of 2.5 mm (9 nm) and emission slit widths of 5 mm (18 nm) were used. An average of 5 individual scans was used to measure excitation and emission spectra.

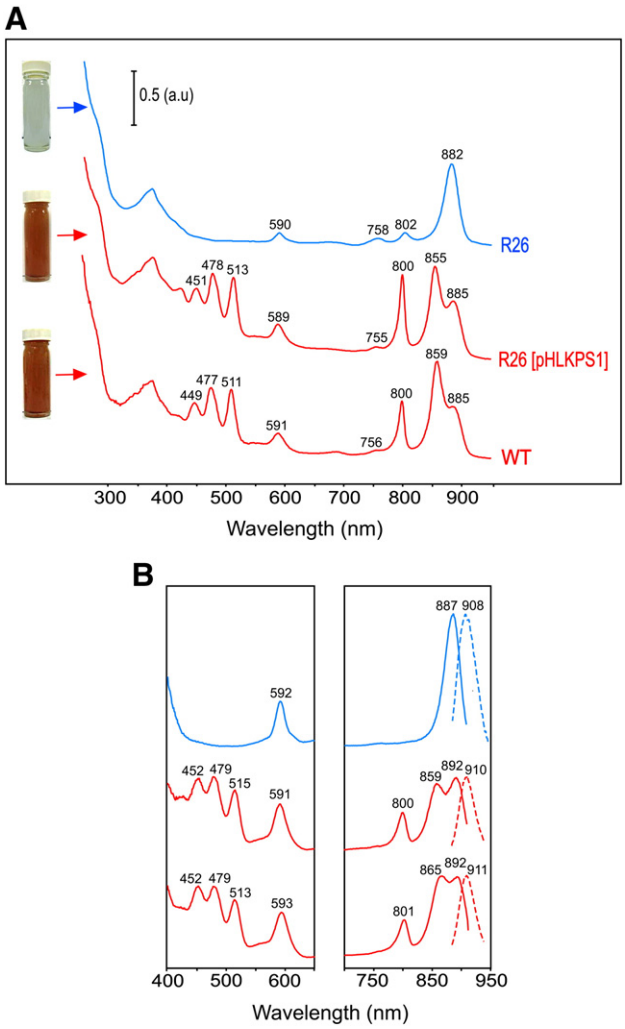

Fig. 2. *In trans* complementation of R-26 with a plasmid-borne *crtB*, encoding phytoene synthase: spectroscopic analysis of ICM from R-26, the complemented strain R-26 [pHLKPS1] and the WT control. (A) A typical photosynthetically grown culture of each strain is shown, with an accompanying absorbance spectrum at 77 K of ICM purified from R-26, the transconjugant strain R-26[pHLKPS1] complemented with *crtB*, and the WT control. The spectra were normalised to the same maximum amplitude in the NIR region of the spectrum. (B) Fluorescence excitation (solid lines) and emission spectra (dashed lines) of ICM purified from R-26 (blue (upper) trace), the transconjugant strain complemented with *crtB*, R-26[pHLKPS1] (red (middle) trace), and the WT control (red (lower) trace). For the excitation spectra fluorescence emission was monitored at 910 nm (left hand panel) and 950 nm (right hand panel). Excitation for the emission spectra was at 590 nm.

2.9. Western blot analysis

Western analysis was performed as described in Ref. [30], with immunodetection using the ECL Detection System (Amersham). Primary antibodies were used in a 1:5000 dilution in blocking solution, and detected using a 1:5000 dilution of horseradish peroxidase-conjugated goat anti-rabbit antiserum as the secondary antibody.

3. Results

3.1. CrtB restores the synthesis and energy transfer functions of carotenoids to mutant R-26

The conjugative plasmid pHLKPS1 restores normal carotenoid synthesis to the carotenoid biosynthesis mutant TC70, in which *crtB*, encoding phytoene synthase, is disrupted by insertion of the transposon

Tn*5* [18]. pHLKPS1 was transferred to R-26, which conferred a brown/red coloration on the normally grey/blue colonies. Examples of the photosynthetically grown cultures are shown in Fig. 2A, together with a WT control. These cultures were scaled up for preparation of purified ICM, which were analysed by absorption spectroscopy at 77 K (Fig. 2A). R-26 showed the well-documented absence of the light-harvesting LH2 complex, apparent through the lack of peaks 800 and 850 nm. The Q_y transition of the carotenoid-less LH1 complex is at 882 nm and peaks corresponding to bacteriopheophytins and the monomeric BChls of the RC were observed at 758 and 802 nm respectively. Comparison of R-26 [pHLKPS1] with R-26 shows the reappearance of carotenoid absorbance peaks at 451, 478 and 513 nm, corresponding to spheroidene (Fig. 2A, middle trace). The LH2 complex, absorbing at 800 and 855 nm is also restored following the introduction of a functional copy of the plasmid-borne *crtB* gene. In terms of the absorbance of carotenoids in the 400–500 nm region, and of LH2 complex BChls at 800 and 850 nm, the transconjugant strain R-26[pHLKPS1] compares well with the WT control in Fig. 2 (lower trace) As a further control, membranes from the *crtB* mutant strain TC70 and the complemented strain TC70[pHLKPS1] were also analysed, giving spectra similar to R-26 and R-26[pHLKPS1] (not shown).

Fluorescence excitation and emission spectra were recorded on ICM prepared from R-26, the transconjugant strain R-26[pHLKPS1] and the WT to determine whether the newly introduced carotenoids were part of a functional light-harvesting system. Fig. 2B (blue line) shows the fluorescence excitation spectrum for R-26, monitoring fluorescence emission at 950 nm from the LH1 complex (Fig. 2B, blue line). There is a maximum in the NIR region at 887 nm and the fluorescence emission maximum for the carotenoid-less LH1 complexes in R-26 occurred at 908 nm, with excitation at 590 nm. The excitation spectra in the 450–520 nm region in Fig. 2B (red lines) correspond well with the absorbance spectra in Fig. 2A, showing that the restored carotenoids in R-26[pHLKPS1] can transfer energy to the LH2 and LH1 BChls, to an extent that compares well with the WT control. Similarly, the excitation spectra for the transconjugant and WT membranes in the NIR region show comparable excitation maxima, at 800 and 859 nm for R-26 [pHLKPS1], and 800 and 865 nm for the WT control. The origin of the 6 nm blue shift in the R-26[pHLKPS1] excitation maximum is not known. Qualitatively, the excitation spectra show that there are comparable levels of energy transfer from the B800 to the B850 BChls within the LH2 complex, and from the LH2 to LH1 complexes in the transconjugant and WT membranes. Since the spectra were recorded at 77 K, the absolute efficiencies of energy transfer are lower than at room temperature, and were not calculated.

Having shown that R-26 is a *crtB* mutant, *crtB* genes were amplified from R-26 and WT 2.4.1 DNA by PCR and sequenced. The 2.4.1. WT was chosen rather than the NCIB 8253 WT used in sequencing the *crtB* gene in Ref. [16], since R-26 was obtained as a result of further mutagenesis of a constitutive high-catalase mutant CC1 [3], assumed to be a derivative of the 2.4.1 WT. Asn 171 is changed to Thr in the primary sequence of CrtB from R-26, a substitution that appears to have inactivated the phytoene synthase in this mutant (see Supplementary Data Fig. S1).

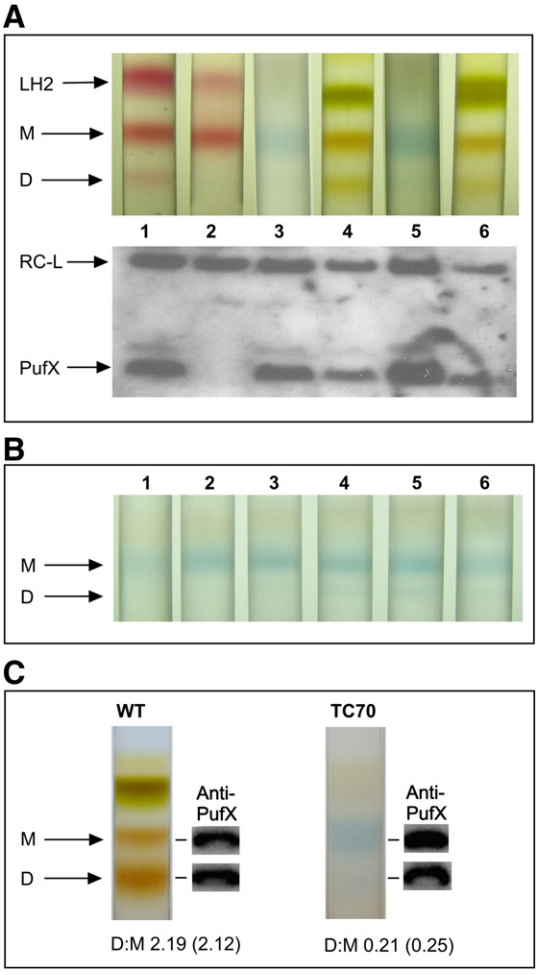

Fig. 3. Analysis of the oligomeric state of RC–LH1–PufX core complexes in the carotenoid-less *crtB* mutants R-26 and TC70. (A) Upper panel: analysis of the presence of LH2 complexes (LH2), core monomers (M) and core dimers (D) on discontinuous sucrose gradients. ICMs were solubilised using β-DDM and the LH2, core monomer and core dimer complexes separated on a sucrose density gradient. The samples were prepared from the following strains: (1) DPF2R[pRHEHX] control; (2) DPF2R[pRHEHX$^-$] control; (3) R-26; (4) R-26 [pHLKPS1]; (5) TC70; (6) TC70 [pHLKPS1]. Lower panel: western blot used to probe the ICM from strains 1–6 as in the upper panel for the presence of PufX, with antibodies to the RC-L subunit used as a loading control. (B) The effects of varying the detergent concentration on the oligomeric state of core complexes solubilised from R-26 ICM. ICMs were solubilised using β-DDM at the following concentrations: (1) 0.1% (2) 0.25% (3) 0.5% (4) 1% (5) 2% (6) 3%. M corresponds to core monomers and D to dimers. (C) Quantitation of the dimer:monomer ratio for the WT and the TC70 mutant. Monomer and dimer fractions were recovered from the gradients and absorbance values at 870 nm, corresponding to the LH1 complex, were extracted from the absorbance spectra. The dimer:monomer ratios in parentheses were estimated separately using densitometry of photographs of the gradients. Next to each band in the two gradients is a western blot, probed with antibodies to the PufX polypeptide.

3.2. Analysis of the oligomeric state of RC–LH1–PufX core complexes in carotenoid-less mutants

The effects of the absence of carotenoids (R-26 and TC70) and their presence (R-26[pHLKPS1] and TC70[pHLKPS1]) were examined in relation to the oligomeric state of the RC–LH1–PufX core complex, which is known to be in a mainly dimeric state in membranes from photosynthetically grown cells [19–21]. ICMs were prepared from photosynthetically grown cells, solubilised using β-DDM and the LH2, core monomer and core dimer complexes separated on a sucrose density gradient. The gradients are shown in Fig. 3A together with a western blot used to probe the ICM for the presence of PufX. The gradients in tubes 1 and 2 were loaded with positive and negative controls, respectively; these are a *puf* operon deletion mutant, DPF2, complemented with a plasmid bearing genes encoding either RC–LH1–PufX (tube 1) or RC–LH1 (tube 2) complexes. The only difference between these samples is the absence of PufX in tube 2, which results in the absence of dimeric RC–LH1–PufX complexes (lowest band), but retention of monomeric cores (middle band) and LH2 (uppermost band). For comparison it was necessary to grow both these strains semi-aerobically in the dark, hence the red colour of the bands. However, it was difficult to grow R-26 semi-aerobically in the dark, so the cells used for the samples in tubes 3–6 were all grown photosynthetically. Tubes 3 and 5 were loaded with R-26 and TC70 ICM, respectively and each showed a band at a position equivalent to the monomer core complex band in the PufX$^-$ control (tube 2). A very

faint band corresponding to dimeric core complexes was also visible in these carotenoid-less mutants. The photosynthetically grown transconjugant strains R-26[pHLKPS1] (tube 4) and TC70[pHLKPS1] (tube 6), each with a functional *crtB* gene, show a banding pattern similar to that of the PufX$^+$ control. Western blot analysis carried out using ICM from each strain shows the presence of the RC-L subunit as a loading control, and also the presence of PufX in all the strains except for the PufX$^-$ control (lane 2). Thus, the loss of core dimers cannot be attributed to a lack of PufX in R-26 or TC70.

Despite this result, it was still possible that carotenoid-less RC–LH1–PufX complexes were in a dimeric state, but with a greater susceptibility to the 3% β-DDM detergent concentration routinely used to solubilise membranes, leading to dissociation into monomers. To check for this possibility ICMs from R-26 were solubilised using 0.1%, 0.25%, 0.5%, 1%, 2%, or 3% β-DDM (Fig. 3B) and analysed as in Fig. 3A. The major band in all the gradients corresponds to monomeric core complexes, with an optimal solubilisation in tubes 3–5 producing the strongest monomer bands and then a decline at 3% β-DDM in tube 6. A faint band corresponding to dimeric core complexes was visible in tubes 4–6, supporting the idea that although monomers are the dominant core complex, there is some evidence for a very small population of dimers as well.

The core dimer:monomer ratios for the WT and the *crtB* mutant TC70, quantified from absorbance spectra of fractions recovered from gradients shown in Fig. 3C, were 2.19 and 0.21, respectively. Densitometry of the gradients gave ratios of 2.12 and 0.25, in reasonable agreement with the fractionation data. Thus, in the wild-type and under the detergent conditions used, approximately 68% of the LH1 is present in core dimers, whereas this figure reduces to approximately 19% in the TC70 *crtB* mutant. Fig. 3C also shows the results of western blotting these monomer and dimer fractions with antibodies to the PufX polypeptide. PufX was present in all cases, so it is likely that in carotenoid-less core complexes PufX is still an integral part of the structure.

In order to verify the oligomeric state of core complexes in mutant R-26, ICMs fractionated on a further sucrose density gradient then analysed by TEM and AFM. Fig. 4A shows TEM images of negatively-stained R-26 membranes, which are vesicles and fragments of membrane mostly ranging from 50 to 150 nm in diameter, with a few larger vesicles. A higher magnification image from an area within Fig. 4A(i) is shown in Fig. 4A(ii); the blue arrow denotes a single-layer membrane with hexagonal patterning of the membrane components. AFM was used to image such a membrane in more detail without the drawbacks of staining and dehydration (Fig. 4B). Low concentrations of β-DDM are normally required to convert spherical WT ICM into membrane patches that flatten onto the mica substrate; however the more lamellar morphology of the R-26 membrane did not necessitate the use of detergent for AFM work. The image of the cytoplasmic face of an R-26 membrane fragment in Fig. 4B shows a hexagonally packed membrane, with the brightest features ascribed to the RC-H subunit, and core complexes lacking the RC (i.e. empty LH1 rings) denoted by blue rings in Fig. 4B (ii). Fig. 4B(iii) shows a height profile analysis across the red lines in Fig. 4B(ii); the average height of the RC-H subunit above the surrounding ring is 1.87 ± 0.24 nm ($n = 11$). Profiles 1–5 allow analysis of the separation of the RC-H protrusions between neighbouring core complexes. These indicate that the majority of core complexes are monomeric, with an average RC–RC separation of 12.2 ± 1.2 nm ($n = 19$). Rare dimeric core complexes were observed (red asterisks) with lower RC–RC separations of 7.5–9.5 nm. For comparison, this same AFM analysis was performed on membrane purified from photosynthetically-grown wild-type *Rba. sphaeroides* (Fig. 4C). Here, rows of dimeric core complexes interspersed by zigzag domains of LH2 complexes are observed. Height profiles 1 and 2, measured across the

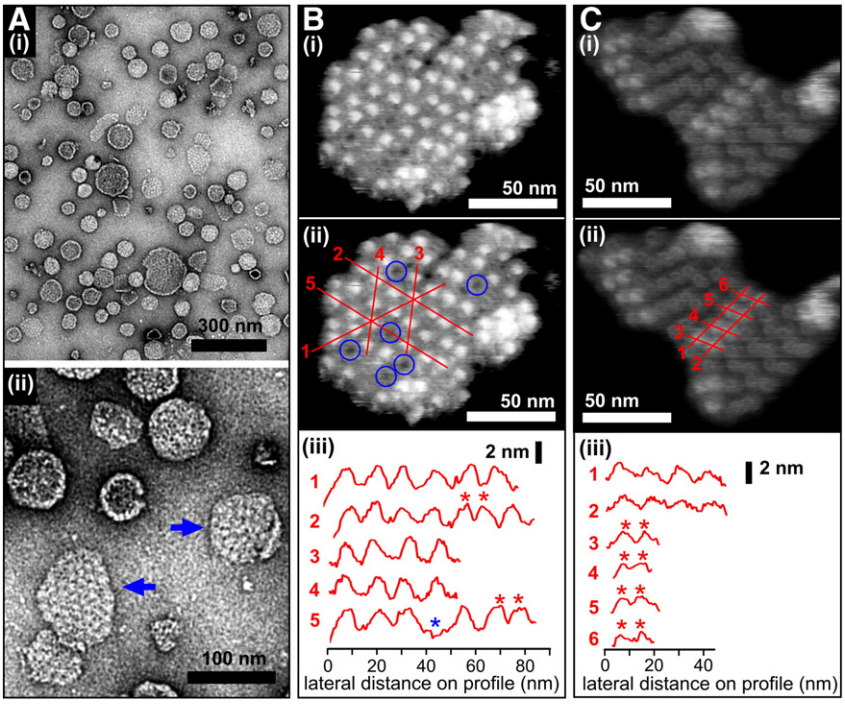

Fig. 4. Analysis of R-26 membranes by TEM and AFM. (A) (i) Negative-stain TEM of R-26 membranes. (ii) Higher magnification image from an area within (i). The blue arrows indicate single membrane layers with hexagonal patterning of the components. (B) (i) Medium resolution AFM image of an R-26 membrane fragment. (ii) Analysis of the image; the blue circles indicate LH1-only rings, lacking the RC. The red lines show the positions of the height profiles drawn at a variety of angles across the membrane surface. (iii) Height profiles 1–5 show the separation of the RC-H protrusions between neighbouring core complexes. The majority of core complexes are monomeric, with an average RC–RC separation of 12.2 ± 1.2 nm ($n = 19$). Red asterisks indicate potentially dimeric core complexes, with RC–RC separations of 7.5–9.5 nm. The blue asterisk denotes the position of an LH1-only complex. (C) (i) AFM analysis of ICM purified from photosynthetically-grown wild-type *Rba. sphaeroides*, as a control. (ii) The same image, but with lines indicating the positions of height profiles; profiles 1 and 2 are measured across the long axis of a row of four dimeric cores and height profiles 3–6 are measured between RCs within individual dimers. (iii) Height profiles 1 and 2 show an inter-dimer RC–RC separation of 12.1 ± 0.4 nm. Height profiles 3–6 show an intra-dimer RC–RC separation of 8.2 ± 0.4 nm. Red asterisks indicate the presence of core dimers.

long axis of a row of four dimeric cores show an inter-dimer RC–RC separation of 12.1 ± 0.4 nm. Height profiles 3–6, measured across individual dimers show an intra-dimer RC–RC separation of 8.2 ± 0.4 nm. These dimensions are consistent with previous measurements of core complexes in wild-type and PufX-minus membranes, where the average separation between RC-H subunits in dimeric RC–LH1–PufX complexes was 7.8 nm, but 12 nm for monomers [30,31].

4. Discussion

The crucial role of carotenoids in photosynthesis was first demonstrated through the analysis of photosynthetic bacteria. Mutants UV-33 and R-26 of *Rba. sphaeroides* were particularly important, and were used to show that carotenoids are essential for preventing photo-oxidative damage, and for light-harvesting [2,5]. R-26 has been used ever since, and there are over two hundred papers on this mutant and the pseudorevertant R-26.1, mainly studies of RC structure and function, but some concentrating on light-harvesting complexes. R-26 was isolated when a high catalase mutant was exposed to ultraviolet light [3]. This procedure appears to have created a series of mutations; firstly there is a high catalase content, then the loss of carotenoids, then a pleiotropic effect on LH2 assembly, which is a consequence of the lack of carotenoids [18]. To this list we can now add another pleiotropic effect, namely the inability to assemble normal levels of dimeric core complexes in the absence of carotenoids.

4.1. Mutations in crtB and other genes in R-26

Carotenoids are restored to R-26 following conjugative transfer of a plasmid bearing a functional *crtB* gene, showing that a lesion in the phytoene synthase step of carotenoid biosynthesis (Fig. 1) is responsible for the blue-green phenotype of R-26. In this respect R-26 has the same properties as the defined *crtB* mutant TC70, where the gene was inactivated through insertion of transposon Tn*5* [16,17,25]. In TC70 the absence of LH2 is a consequence of a requirement for carotenoids in the assembly pathway for this complex; this was demonstrated by a pulse-chase radiolabeling experiment, which showed that although LH2 polypeptides were synthesised they were not stably incorporated into the TC70 membrane [18]. Similarly, a lesion in *crtI* encoding phytoene desaturase (Fig. 1) abolishes LH2 assembly and complementation of a *crtI* mutant with a plasmid-borne copy of *crtI* restored carotenoid biosynthesis and allowed the stable assembly of LH2 into the ICM [18]. The fact that *crtB* restores normal levels of LH2 assembly to the trans-conjugant strain R-26[pHLKPS1] shows that it is not the Val24 → Phe substitution in the LH2 α-subunit in R-26 [32] that prevents LH2 assembly in R-26. Furthermore the fluorescence excitation spectra in Fig. 2 show that the full pathway of excitation energy transfer from carotenoids to BChls, and from LH2 to LH1, has been restored to R-26 [pHLKPS1], so the Leu30 → Pro mutation in the LH1 β-subunit of R-26 [33] does not affect these processes.

The presence of mutations in genes encoding the LH1 complex in R-26 [33] makes this mutant less than ideal for studies of light-harvesting structure and function, given the lack of carotenoids as well. This is particularly true for R-26.1, a partial revertant of R-26 [34] which still lacks carotenoids but has, in addition to LH1, a pseudo-LH2 complex with no B800 absorbance band and a red-shifted absorbance maximum at approximately 860 nm. Here, multiple mutations are present including a Val24 → Phe substitution in the LH2 α-subunit, a Val22 → Ala substitution in the LH1 α-subunit and a Leu30 → Pro substitution in the LH1 β-subunit [33]. The mutation Val24 → Phe in the LH2 α-subunit of R-26.1 had already been identified many years previously by sequencing the LH2 polypeptide [32]. This mutation was apparently inherited from the parental R-26 strain. It is not clear why a carotenoid-less LH2 complex is able to assemble in R-26.1 but not R-26; as pointed out by Robert et al. [35] R-26.1 is a partial suppressor mutation and it could have arisen through a mutation in the biosynthetic pathway for LH2 complexes. One candidate for the suppressor effect could be a mutation in *pucC* encoding the LH2 assembly complex [36], so the LH2 assembly pathway is able to tolerate the loss of carotenoids.

4.2. The pleiotropic effect of loss of carotenoids on the formation of RC–LH1–PufX dimers

Mutants that have no LH2 complexes but retain dimeric core complexes assemble tubular ICM [20,37,38], as a consequence of the dimeric nature of the core complex, and its shallow "V" shape, which imposes curvature on the membrane in which it sits [39,40]. The membranes purified from R-26 were small vesicles and patches (Fig. 4A, B), offering a clue as to the other pleiotropic effect of the lack of carotenoids, namely that these pigments are required for efficient dimerisation of core complexes, and in their absence mainly monomers form which have lost their strong membrane-curving properties. Inspection of sucrose density gradients (Fig. 3) and AFM topographs (Fig. 4) verifies that carotenoid-less RC–LH1 complexes are present almost entirely as monomers, an effect also produced by truncating the N-terminus of PufX, or removing it altogether [30,41]. This monomeric state in R-26 contrasts with the dimeric cores observed in membranes from the WT (Fig. 4C). We note that no detergent treatment was necessary to produce R-26 membranes suitable for AFM, in contrast to the requirement for low concentrations of β-DDM to open out spherical WT ICM vesicles on the mica substrate prior to AFM imaging. The presence of core dimers is a characteristic of membranes from photosynthetically grown cells of the WT, whether these membranes are treated with detergent, or not, as in the case of the biosynthetic precursor UPB membranes from the WT [31]. A further point to note is that the sucrose density gradients in Fig. 3, as well as the AFM in Ref. [31], show that some core monomers are also present in WT membranes, even though dimers predominate.

The western blots in Fig. 3 show that PufX is present in both R-26 and TC70 membranes, and also that PufX is present in the partially purified monomeric, carotenoid-less RC–LH1–PufX complexes so the monomeric character of these complexes cannot be attributed to a lack of PufX. We conclude that there is a direct requirement for carotenoids for the efficient dimerisation of RC–LH1–PufX complexes, demonstrating yet another role for these pigments in the assembly and function of this bacterial photosystem.

It has been known for a long time that there is a relatively high content of carotenoid in the LH1 complex; it was suggested that the minimal LH1 complex was composed of two polypeptides, two BChls and two carotenoids [23]. The structural information available for the RC–LH1–PufX dimer [22,39] implies 56 LH1 BChls and therefore 56 carotenoids per complex, with the carotenoids likely to provide structural support as well as extra capabilities for light absorption and photo-protection. Certainly, carotenoids have been found to enhance the reconstitution of LH1-only complexes from the separate polypeptide, BChl and carotenoid components [42,43]. Studies of mutants of *Rba. capsulatus* show that there is an interrelationship between carotenoids, PufX and dimerisation of the core complex, and it has been proposed that PufX affects multiple carotenoid binding sites in LH1 [44].

4.3. Effects of the loss of carotenoids on the morphology and function of photosynthetic membranes

The cell ultrastructure of R-26 was first reported by Lommen and Takemoto [45], who observed some spherical vesicles as well as flattened lamellar membranes in thin sections and freeze-fracture preparations of R-26 cells. Thus, mutations early in the carotenoid pathway, at the level of phytoene synthase and phytoene desaturase, affect the morphology of ICM of *Rba. sphaeroides*. A systematic survey of the effects of each step in the carotenoid pathway on membrane morphology revealed that the decisive step for normal membrane

assembly is the formation of neurosporene from phytoene, catalysed by the three-step phytoene desaturase [18]. Interestingly, this study showed that relatively small amounts of ICM accumulate in TC70, the *crtB* mutant, whereas layers of lamellar membranes are observed in the *crtI* mutant, TC72. It appears that the formation of phytoene is able to promote some membrane and photosystem assembly, implying that this colourless carotenoid can be incorporated into light-harvesting complexes to some degree. Having established that carotenoids at the level of neurosporene and beyond are important for the assembly of both LH2 [18] and RC–LH1–PufX dimers it is possible to explain the observations of Lommen and Takemoto [45], and those of Lang et al. [18] on cell ultrastructure: spherical ICM become the dominant membrane structures within the cell when normal carotenoid biosynthesis permits the assembly of both the LH2 and the membrane-curving core dimer complexes.

The AFM topographs of R-26 membranes show that they are largely composed of hexagonally packed monomeric complexes. Of the 27 RC–LH1 complexes analysed only two dimers were found, which is less than the proportion of dimers found in sucrose gradient analysis of detergent-treated TC70 samples in Fig. 3C. Both monomeric and dimeric cores from TC70 contain PufX, as shown by the western blots in Fig. 3. Thus, the absence of carotenoids from core complexes favours the assembly of core monomers and overrides the normal dimerising effect of PufX, driven by the N-terminal domain of this polypeptide [30,41]. R-26 membranes ranged from 50 to 150 nm in size, which is sufficient to accommodate approximately 25–200 RC–LH1–PufX core monomers, containing between 750 and 6,000 LH1 BChls. This can be compared to ICM vesicles from the WT bacterium, the most representative of which have been modelled to contain approximately 4,500 BChls, 100 LH2 complexes and 18 dimeric RC–LH1–PufX complexes [46,47]. A recent investigation of excitation transfer connectivity compared membranes from R-26 and several other mutants of *Rba. sphaeroides* [33]. It was found that the LH1:RC ratio is doubled in R-26 in comparison with other mutants lacking LH2, and the authors also calculated a surprisingly high value for the connectivity parameter *J*, which they suggested could arise from "excess" LH1 complexes inserted between RC–LH1 complexes. It is therefore interesting that the AFM topographs in Fig. 4 reveal some empty LH1 rings interspersed among the monomeric core complexes, although we cannot exclude the possibility that RCs were removed from some of the LH1 rings by the AFM. It is also possible that because of the relatively gentle tapping mode AFM employed, the presence of a few LH1 rings lacking RCs reflects the real situation in the membrane. In the example in Fig. 4 there are approximately 70 LH1 rings in total representing 2,100 LH1 BChls, at 30 BChls per monomeric ring, assuming interruption with PufX as in the RC–LH1–PufW structure [48]. Of these, approximately 10 "empty" LH1 rings can be identified. This is just one membrane, whereas the measurements of De Rivoyre et al. [33] are bulk measurements, but nevertheless there is some correspondence between their suggestion and our AFM data. AFM support for their further suggestion, that a small fraction of the LH1 antenna could reside in a domain disconnected from the rest of the complexes, might require imaging smaller membrane fragments, which is technically more demanding.

In conclusion, this work has demonstrated that as well as being reliant upon the presence of PufX, which was already known, efficient dimerisation of core complexes also requires carotenoids. Future work will examine the effects of varying the type of carotenoid on the dimerisation process.

Supplementary materials related to this article can be found online at doi:10.1016/j.bbabio.2011.05.020.

Acknowledgements

C.N.H., C.V., E.C.M., H.P.L. and J.D.T. acknowledge financial support from the Biotechnology and Biological Sciences Research Council (UK). C.N.H. was supported as part of the Photosynthetic Antenna Research Center (PARC), an Energy Frontier Research Center funded by the U.S. Department of Energy, Office of Science, Office of Basic Energy Sciences under award number DE-SC 0001035. I.W.N., P.G.A. and D.J.M. were all supported by doctoral studentships from the Biotechnology and Biological Sciences Research Council (UK).

References

[1] J.B. Thomas, On the role of carotenoids in photosynthesis in *Rhodospirillum rubrum*, Biochim. Biophys. Acta 5 (1950) 186–196.
[2] W.R. Sistrom, M. Griffiths, R.Y. Stanier, The biology of a photosynthetic bacterium which lacks coloured carotenoids, J. Cell. Comp. Physiol. 48 (1956) 473–516.
[3] R.K. Clayton, C. Smith, *Rhodopseudomonas spheroides*: high catalase and blue-green double mutants, Biochem. Biophys. Res. Commun. 3 (1960) 143–145.
[4] L.N.M. Duysens, W.J. Huiskamp, J.J. Vos, J.M. van der Hart, Reversible changes in bacteriochlorophyll in purple bacteria upon illumination, Biochim. Biophys. Acta 19 (1956) 188–190.
[5] R.K. Clayton, Primary reactions in bacterial photosynthesis. I. The nature of light-induced absorbancy changes in chromatophores; evidence for a special bacteriochlorophyll component. Photochem. Photobiol. 1 (1962) 201–210.
[6] R.K. Clayton, Towards the isolation of a photochemical reaction center in *Rhodopseudomonas spheroides*, Biochim. Biophys. Acta 75 (1963) 312–323.
[7] R.K.Clayton, R.T.Wang, Photochemical reaction centers from *Rhodopseudomonas spheroides*, (1971) 696–704.
[8] G. Feher, Some chemical and physical properties of a bacterial reaction center particle and its primary photochemical reactants, Photochem. Photobiol. 14 (1971) 373–387.
[9] J.P. Allen, G. Feher, T.O. Yeates, H. Komiya, D.C. Rees, Structure of the reaction center from *Rhodobacter sphaeroides* R-26: the protein subunits, Proc. Natl. Acad. Sci. USA 84 (1987) 6162–6166.
[10] J.P. Allen, G. Feher, T.O. Yeates, H. Komiya, D.C. Rees, Structure of the reaction center from *Rhodobacter sphaeroides* R-26: the cofactors, Proc. Natl. Acad. Sci. USA 84 (1987) 5730–5734.
[11] T.O. Yeates, H. Komiya, D.C. Rees, J.P. Allen, G. Feher, Structure of the reaction center from *Rhodobacter sphaeroides* R-26: membrane–protein interactions, Proc. Natl. Acad. Sci. USA 84 (1987) 6438–6442.
[12] J. Deisenhofer, O. Epp, K. Miki, R. Huber, H. Michel, Structure of the protein subunits in the photosynthetic reaction centre of *Rhodopseudomonas viridis* at 3 Å resolution, Nature 318 (1985) 618–624.
[13] J.D. Bolt, K. Sauer, Fluorescence properties of the light-harvesting bacteriochlorophyll protein from *Rhodopseudomonas sphaeroides* R-26, Biochim. Biophys. Acta 637 (1981) 342–347.
[14] M. Griffiths, R.Y. Stanier, Some mutational changes in the photosynthetic pigment system of *Rhodopseudomonas spheroides*, J. Gen. Microbiol. 14 (1956) 715.
[15] J. Zurdo, C.C. Fernandez, J.M. Ramirez, A structural role of the carotenoid in the light-harvesting II protein of *Rhodobacter capsulatus*, Biochem. J. 290 (1993) 531–537.
[16] H.P. Lang, R.J. Cogdell, A.T. Gardiner, C.N. Hunter, Early steps in carotenoid biosynthesis: sequences and transcriptional analysis of the *crtI* and *crtB* genes of *Rhodobacter sphaeroides* and overexpression and reactivation of *crtI* in *Escherichia coli* and *R. sphaeroides*, J. Bacteriol. 176 (1994) 3859–3869.
[17] H.P. Lang, R.J. Cogdell, S. Takaichi, C.N. Hunter, Complete DNA sequence, specific Tn*5* insertion map, and gene assignment of the carotenoid biosynthesis pathway of *Rhodobacter sphaeroides*, J. Bacteriol. 177 (1995) 2064–2073.
[18] H.P. Lang, C.N. Hunter, The relationship between carotenoid biosynthesis and the assembly of the light-harvesting LH2 complex in *Rhodobacter sphaeroides*, Biochem. J. 298 (1994) 197–205.
[19] C. Jungas, J.L. Ranck, J.L. Rigaud, P. Joliot, A. Verméglio, Supramolecular organization of the photosynthetic apparatus of *Rhodobacter sphaeroides*, EMBO J. 18 (1999) 534–542.
[20] W.H.J. Westerhuis, J.N. Sturgis, E.C. Ratcliffe, C.N. Hunter, R.A. Niederman, Isolation, size estimates, and spectral heterogeneity of an oligomeric series of light-harvesting 1 complexes from *Rhodobacter sphaeroides*, Biochemistry 41 (2002) 8698–8707.
[21] C.A. Siebert, P. Qian, D. Fotiadis, A. Engel, C.N. Hunter, P.A. Bullough, Molecular architecture of photosynthetic membranes in *Rhodobacter sphaeroides*: the role of PufX, EMBO J. 23 (2004) 690–700.
[22] P. Qian, C.N. Hunter, P.A. Bullough, The 8.5 Å projection structure of the core RC–LH1–PufX dimer of *Rhodobacter sphaeroides*, J. Mol. Biol. 349 (2005) 948–960.
[23] R.M. Broglie, C.N. Hunter, P. Delepelaire, R.A. Niederman, N.H. Chua, R.K. Clayton, Isolation and characterization of the pigment–protein complexes of *Rhodopseudomonas sphaeroides* by lithium dodecyl sulfate/polyacrylamide gel electrophoresis, Proc. Natl. Acad. Sci. USA 77 (1980) 87–91.
[24] S.A. Coomber, C.N. Hunter, Construction of a physical map of the 45 kb photosynthetic gene cluster of *Rhodobacter sphaeroides*, Arch. Microbiol. 151 (1989) 454–458.
[25] S.A. Coomber, M. Chaudhri, A. Connor, G. Britton, C.N. Hunter, Localized transposon Tn*5* mutagenesis of the photosynthetic gene cluster of *Rhodobacter sphaeroides*, Mol. Microbiol. 4 (1990) 977–989.
[26] G.W. Naylor, H.A. Addlesee, L.C.D. Gibson, C.N. Hunter, The photosynthesis gene cluster of *Rhodobacter sphaeroides*, Photosyn. Res. 62 (1999) 121–139.
[27] G.A. Armstrong, Genetics of eubacterial carotenoid biosynthesis: a colorful tale, Ann. Rev. Microbiol. 51 (1997) 629–659.

[28] C.N. Hunter, B.S. Hundle, J.E. Hearst, H.P. Lang, A.T. Gardiner, S. Takaichi, R.J. Cogdell, Introduction of new carotenoids into the bacterial photosynthetic apparatus by combining the carotenoid biosynthetic pathways of *Erwinia herbicola* and *Rhodobacter sphaeroides*, J. Bacteriol. 176 (1994) 3692–3697.
[29] C.N. Hunter, G. Turner, Transfer of genes coding for apoproteins of reaction center and light-harvesting LH1 complexes to *Rhodobacter sphaeroides*, J. Gen. Microbiol. 134 (1988) 1471–1480.
[30] E.C. Ratcliffe, R.B. Tunnicliffe, I.W. Ng, P.G. Adams, P. Qian, K. Holden-Dye, M.R. Jones, M.P. Williamson, C.N. Hunter, Experimental evidence that the membrane-spanning helix of PufX adopts a bent conformation that facilitates dimerisation of the Rhodobacter sphaeroides RC–LH1 complex through N-terminal interactions, Biochim. Biophys. Acta 1807 (2011) 95–107.
[31] J.D. Tucker, C.A. Siebert, M. Escalante, P.G. Adams, J.D. Olsen, C. Otto, D.L. Stokes, C.N. Hunter, Membrane invagination in *Rhodobacter sphaeroides* is initiated at curved regions of the cytoplasmic membrane, then forms both budded and fully detached spherical vesicles, Mol. Microbiol. 76 (2010) 833–847.
[32] R. Theiler, F. Stuer, H. Zuber, R.J. Cogdell, A comparison of the primary structures of the two B800-850 apoproteins from wild-type *Rhodopseudomonas sphaeroides* strain 2.4.1 and a carotenoid-less mutant strain R26.1, FEBS Lett. 175 (1984) 231–237.
[33] M. De Rivoyre, N. Ginet, P. Bouyer, J. Lavergne, Excitation transfer connectivity in different purple bacteria: a theoretical and experimental study, Biochim. Biophys. Acta 1797 (2010) 1780–1794.
[34] E. Davidson, R.J. Cogdell, Reconstitution of carotenoids into the light-harvesting pigment–protein complex from the carotenoidless mutant of *Rhodopseudomonas sphaeroides* R26, Biochim. Biophys. Acta 635 (1981) 295–303.
[35] B. Robert, A. Verméglio, M. Lutz, Structural characterization and comparison of antenna complexes of R26 and R26.1 mutants of *Rhodopseudomonas sphaeroides*, Biochim. Biophys. Acta 766 (1984) 259–262.
[36] L.C.D. Gibson, P. McGlynn, M. Chaudhri, C.N. Hunter, A putative anaerobic coproporphyrinogen III oxidase in *Rhodobacter sphaeroides*. II. Analysis of a region of the genome encoding *hemF* and the *puc* operon, Mol. Microbiol. 6 (1992) 3171–3186.
[37] C.N. Hunter, J.D. Pennoyer, J.N. Sturgis, D. Farrelly, R.A. Niederman, Oligomerization states and associations of light-harvesting pigment protein complexes of *Rhodobacter sphaeroides* as analyzed by lithium dodecyl-sulfate polyacrylamide-gel electrophoresis, Biochemistry 27 (1988) 3459–3467.
[38] P.J. Kiley, A.R. Varga, S. Kaplan, Physiological and structural analysis of light-harvesting mutants of *Rhodobacter sphaeroides*, J. Bacteriol. 170 (1988) 1103–1115.
[39] P. Qian, P. Bullough, C.N. Hunter, Three-dimensional reconstruction of a membrane-bending complex, J. Biol. Chem. 283 (2008) 14002–14011.
[40] J. Hsin, J. Gumbart, L.G. Trabuco, E. Villa, P. Qian, C.N. Hunter, K. Schulten, Protein-induced membrane curvature investigated through molecular dynamics flexible fitting, Biophys. J. 97 (2009) 321–329.
[41] F. Francia, J. Wang, H. Zischka, G. Venturoli, D. Oesterhelt, Role of the N- and C-terminal regions of the PufX protein in the structural organization of the photosynthetic core complex of *Rhodobacter sphaeroides*, Eur. J. Biochem. 269 (2002) 1877–1885.
[42] C.M. Davis, P.L. Bustamante, P.A. Loach, Reconstitution of the bacterial core light-harvesting complexes of *Rhodobacter sphaeroides* and *Rhodospirillum rubrum* with isolated a- and b-polypeptides, bacteriochlorophyll *a*, and carotenoid, J. Biol. Chem. 270 (1995) 5793–5804.
[43] L. Fiedor, J. Akahane, Y. Koyama, Carotenoid-induced cooperative formation of bacterial photosynthetic LH1 complex, Biochemistry 43 (2004) 16487–16496.
[44] M. Aklujkar, J.T. Beatty, The PufX protein of *Rhodobacter capsulatus* affects the properties of bacteriochlorophyll *a* and carotenoid pigments of light-harvesting complex 1, Arch. Biochem. Biophys. 443 (2005) 21–32.
[45] M.A.J. Lommen, J.T. Takemoto, Ultrastructure of carotenoid mutant strain R-26 of *Rhodopseudomonas sphaeroides*, Arch. Microbiol. 118 (1978) 305–308.
[46] M.K. Şener, J.D. Olsen, C.N. Hunter, K. Schulten, Atomic level structural and functional model of a bacterial photosynthetic membrane vesicle, Proc. Natl. Acad. Sci. USA 104 (2007) 15273–15278.
[47] M. Şener, J. Strumpfer, J.A. Timney, A. Freiberg, C.N. Hunter, K. Schulten, Photosynthetic vesicle architecture and constraints on efficient energy harvesting, Biophys. J. 99 (2010) 67–75.
[48] A.W. Roszak, T.D. Howard, J. Southall, A.T. Gardiner, C.J. Law, N.W. Isaacs, R.J. Cogdell, Crystal structure of the RC–LH1 core complex from *Rhodopseudomonas palustris*, Science 302 (2003) 1969–1972.
[49] G. Garcia-Asua, H.P. Lang, R.J. Cogdell, C.N. Hunter, Carotenoid diversity: a modular role for the phytoene desaturase step, Trends Plant Sci. 3 (1998) 445–449.
[50] S. Takaichi, Distribution and biosynthesis of carotenoids, in: C.N. Hunter, F. Daldal, M.C. Thurnauer, J.T. Beatty (Eds.), The purple phototrophic bacteria, Springer, Dordrecht, The Netherlands, 2009, pp. 97–117.